Report on Studies of the Effect on Resolution of the Exit Window of the HRS Spectrometers in Hall A

by John J. LeRose

1/7/00
JLab-TN-00-001

Abstract

This note reports on the results of a study made of the improvements in momentum, position, and angular resolution gained by replacing the standard 4 mil Ti spectrometer exit window with a much thinner window (factor of ten reduction in radiation length) as used on the spectrometers in Mainz (Institut für Kernphysik, Johannes Gutenberg-Universität). Only effects of multiple scattering in the exit window, the following vertical drift chamber array with intervening layers of air, and the intrinsic resolution of the drift chambers themselves are considered. Improvements are found to be minimal.

Spectrometer Exit window and VDC layout:

Details of the exit window and VDC layout are shown below in Figure 1.

Figure 1

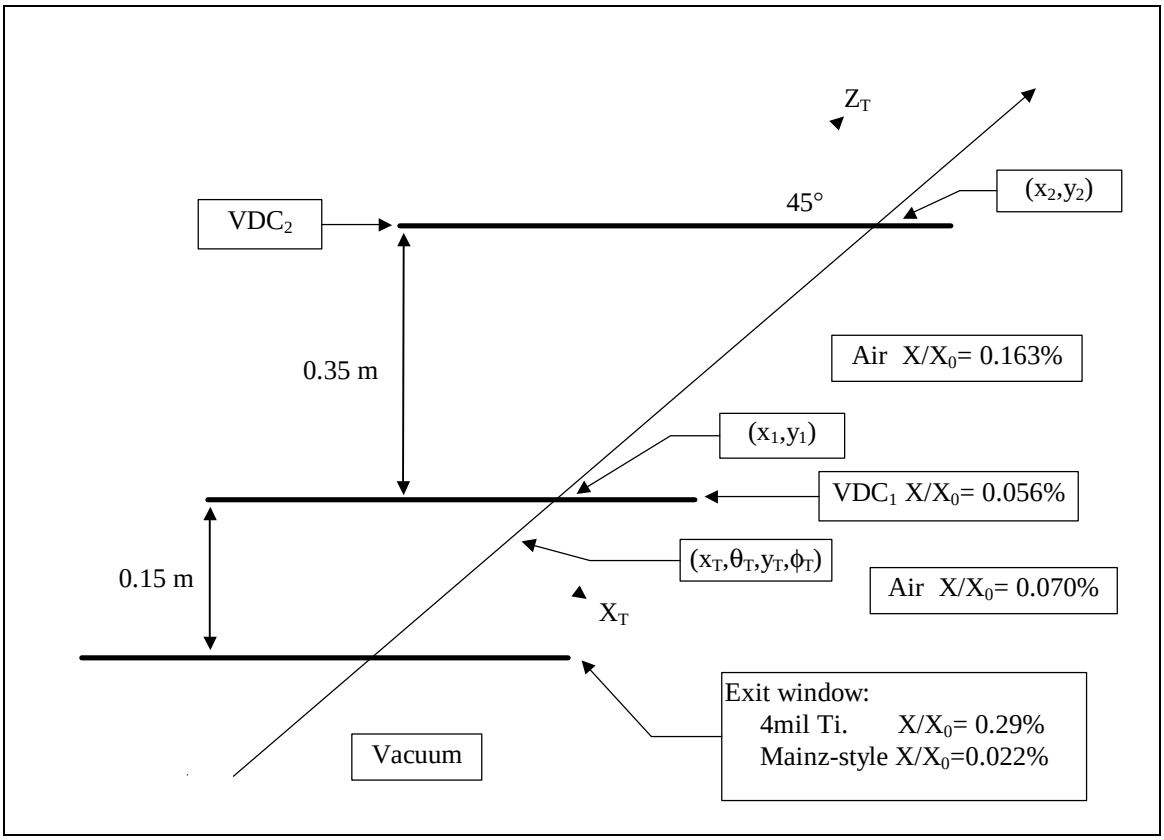

General Scheme:

1. For representative trajectories ($x_0 = \theta_0 = y_0 = \phi_0 = 0$, and δ = -4.5%, -2.25%, 0%, 2.25%, 4.5%), **e.g.** dash-dot line in figure 1 above, errors in x_i,y_i (trajectory coordinates as it passes through VDC_1 or VDC_2) resulting from multiple scattering in the exit window, the air between the exit window and VDC_1, VDC_1 itself, and the air between VDC_1 and VDC_2 are evaluated. (Intrinsic resolution of the VDC's is included).
2. These errors are translated into errors in the TRANSPORT coordinates $(x_T,\theta_T,y_T,\phi_T)$.
3. The errors in $(x_T,\theta_T,y_T,\phi_T)$ are applied in a Monte Carlo fashion to large sets of trajectories at each of the δ values mentioned above and otherwise spanning the acceptance of the specrometer. (**i.e.** the value of each coordinate is altered using a gaussian random generator with sigmas determined in step 2). These altered trajectories are fed through the spectrometer reconstruction matrices to determine the target parameters (δ, θ_0, y_0, ϕ_0). The difference between these and the original, known values for each trajectory are stored in histograms and the standard deviation (σ_i) for each target parameter is evaluated.

Evaluation of Measurement Errors:

The first step in calculating the measurement error is the evaluation of the multiple scattering in each of the relevant layers of material in the detector stack starting at the exit window. In particular, four sources of multiple scattering are considered:

1. The exit window
2. The air layer between the exit window and VDC_1

3. VDC_1
4. The air layer between VDC_1 and VDC_2

Multiple scattering in each layer is characterised by a multiple scattering angle given by the standard expression[1]:

$$\theta_0 = \frac{13.6\ \text{MeV}}{\beta cp} z \sqrt{\frac{X}{X_0}} \left[1 + 0.038 \ln\left(\frac{X}{X_0}\right)\right]$$

Errors (σ's) for position determination of trajectories $\sigma_{x1,y1}$ and $\sigma_{x2,y2}$ for $VDC_1$and VDC_2 are the determined by the following expessions:

$$\sigma_{x1,y1} = \sqrt{(\theta_1 l_1)^2 + (\tfrac{1}{\sqrt{3}}\theta_2 l_1)^2 + (\sigma_{VDC})^2}$$

$$\sigma_{x2,y2} = \sqrt{(\sigma_{x1,y1})^2 + (\theta_3 l_2)^2 + (\tfrac{1}{\sqrt{3}}\theta_4 l_2)^2 + (\sigma_{VDC})^2}$$

Here θ_j refers to each of the layers enumerated above, l_1 is the distance along the optical axis between the exit window and VDC_1, and l_2 is the distance along the optical axis between the VDC_i's. σ_{VDC} is the intrinsic resolution of the VDC_i's (100 μm).

The $\sigma_{xi,yi}$'s are then converted into errors on x_T,θ_T,y_T,ϕ_T (dashed line in figure 1). In general, this conversion depends on each particular trajectory. For this study, it was decided to evaluate those errors on x_T,θ_T,y_T,ϕ_T for five representative trajectories, $x_0 = \theta_0 = y_0 = \phi_0 = 0$, and δ = -4.5%, -2.25%, 0, 2.25%, and 4.5%. Results for electrons and protons for various values of P_0 are tabulated below for both the Ti (thick) and Mainz-style[2] (thin) window (units are meters and radians).

Ti window		**electrons**				**protons**			
P (MeV/c)	δ	σx_t	$\sigma\theta_t$	σy_t	$\sigma\phi_t$	σx_t	$\sigma\theta_t$	σy_t	$\sigma\phi_t$
800	-4.50%	0.00040	0.00073	0.00052	0.00095	0.00056	0.00103	0.00072	0.00133
	-2.25%	0.00017	0.00067	0.00024	0.00091	0.00025	0.00094	0.00033	0.00127
	0.00%	0.00013	0.00061	0.00018	0.00087	0.00018	0.00086	0.00026	0.00122
	2.25%	0.00027	0.00056	0.00041	0.00083	0.00039	0.00079	0.00057	0.00117
	4.50%	0.00042	0.00052	0.00065	0.00080	0.00059	0.00073	0.00091	0.00112
1000	-4.50%	0.00035	0.00064	0.00045	0.00082	0.00043	0.00079	0.00055	0.00102
	-2.25%	0.00015	0.00058	0.00020	0.00078	0.00019	0.00072	0.00025	0.00097
	0.00%	0.00011	0.00053	0.00016	0.00075	0.00014	0.00066	0.00020	0.00093
	2.25%	0.00024	0.00049	0.00035	0.00072	0.00029	0.00060	0.00043	0.00089
	4.50%	0.00036	0.00045	0.00056	0.00069	0.00045	0.00056	0.00069	0.00085
2000	-4.50%	0.00026	0.00047	0.00033	0.00061	0.00026	0.00048	0.00034	0.00063
	-2.25%	0.00011	0.00043	0.00015	0.00058	0.00012	0.00044	0.00016	0.00060
	0.00%	0.00008	0.00039	0.00012	0.00055	0.00009	0.00040	0.00012	0.00057
	2.25%	0.00018	0.00036	0.00026	0.00053	0.00018	0.00037	0.00027	0.00055
	4.50%	0.00027	0.00033	0.00041	0.00051	0.00028	0.00034	0.00042	0.00053
3000	-4.50%	0.00024	0.00043	0.00030	0.00056	0.00024	0.00044	0.00031	0.00056
	-2.25%	0.00010	0.00039	0.00014	0.00053	0.00010	0.00040	0.00014	0.00054
	0.00%	0.00008	0.00036	0.00011	0.00051	0.00008	0.00036	0.00011	0.00051
	2.25%	0.00016	0.00033	0.00024	0.00049	0.00016	0.00033	0.00024	0.00049
	4.50%	0.00025	0.00031	0.00038	0.00047	0.00025	0.00031	0.00038	0.00047
4000	-4.50%	0.00023	0.00042	0.00029	0.00054	0.00023	0.00042	0.00030	0.00054
	-2.25%	0.00010	0.00038	0.00013	0.00052	0.00010	0.00038	0.00014	0.00052
	0.00%	0.00007	0.00035	0.00010	0.00049	0.00007	0.00035	0.00010	0.00050
	2.25%	0.00016	0.00032	0.00023	0.00047	0.00016	0.00032	0.00023	0.00047
	4.50%	0.00024	0.00030	0.00037	0.00045	0.00024	0.00030	0.00037	0.00046

Mainz		electrons				protons			
P (MeV/c)	δ	σx_t	$\sigma\theta_t$	σy_t	$\sigma\phi_t$	σx_t	$\sigma\theta_t$	σy_t	$\sigma\phi_t$
800	-4.50%	0.00032	0.00056	0.00042	0.00073	0.00043	0.00073	0.00056	0.00094
	-2.25%	0.00014	0.00051	0.00020	0.00069	0.00019	0.00067	0.00026	0.00090
	0.00%	0.00008	0.00047	0.00011	0.00066	0.00009	0.00061	0.00013	0.00086
	2.25%	0.00019	0.00043	0.00028	0.00064	0.00023	0.00056	0.00034	0.00083
	4.50%	0.00030	0.00040	0.00046	0.00061	0.00038	0.00052	0.00058	0.00079
1000	-4.50%	0.00029	0.00051	0.00038	0.00066	0.00034	0.00059	0.00044	0.00076
	-2.25%	0.00013	0.00047	0.00017	0.00063	0.00015	0.00054	0.00021	0.00073
	0.00%	0.00008	0.00043	0.00011	0.00060	0.00008	0.00049	0.00012	0.00070
	2.25%	0.00018	0.00039	0.00026	0.00058	0.00020	0.00045	0.00029	0.00067
	4.50%	0.00028	0.00036	0.00043	0.00055	0.00031	0.00042	0.00048	0.00064
2000	-4.50%	0.00024	0.00043	0.00031	0.00056	0.00024	0.00044	0.00031	0.00056
	-2.25%	0.00010	0.00039	0.00014	0.00053	0.00011	0.00040	0.00014	0.00054
	0.00%	0.00007	0.00036	0.00010	0.00051	0.00007	0.00036	0.00010	0.00052
	2.25%	0.00016	0.00033	0.00023	0.00049	0.00016	0.00033	0.00023	0.00049
	4.50%	0.00024	0.00030	0.00037	0.00047	0.00024	0.00031	0.00038	0.00047
3000	-4.50%	0.00023	0.00041	0.00029	0.00053	0.00023	0.00042	0.00029	0.00054
	-2.25%	0.00010	0.00038	0.00013	0.00051	0.00010	0.00038	0.00014	0.00051
	0.00%	0.00007	0.00035	0.00010	0.00049	0.00007	0.00035	0.00010	0.00049
	2.25%	0.00015	0.00032	0.00022	0.00047	0.00015	0.00032	0.00023	0.00047
	4.50%	0.00023	0.00029	0.00036	0.00045	0.00023	0.00029	0.00036	0.00045
4000	-4.50%	0.00022	0.00041	0.00029	0.00053	0.00022	0.00041	0.00029	0.00053
	-2.25%	0.00010	0.00037	0.00013	0.00050	0.00010	0.00037	0.00013	0.00050
	0.00%	0.00007	0.00034	0.00010	0.00048	0.00007	0.00034	0.00010	0.00048
	2.25%	0.00015	0.00031	0.00022	0.00046	0.00015	0.00031	0.00022	0.00046
	4.50%	0.00023	0.00029	0.00036	0.00044	0.00023	0.00029	0.00036	0.00044

Spectrometer Model:

A SNAKE[3]-based prescription is used to describe the spectrometer. In the model of the spectrometer used an analytic calculation of the magnetic fields in the quadrupoles and dipoles is employed. In the case of the quadrupoles the effective length and field strength used is that determined by the QMM quadrupole field mapping[4] with fringing fields described by the expression:

$$G(z) = \frac{G_0}{1 + e^{S(z)}}$$

$$S(z) = \sum_{i=0}^{5} S_i \left(\frac{z}{D}\right)^i$$

G_0 is the field gradient at the center of the magnet. D is the diameter of the quadrupole and z is the displacement along the axis of the magnet from the effective field boundary (z always points outward from the magnet).

A generic set of values given below for S_i's was used.

S_0	S_1	S_2	S_3	S_4	S_4
0.1039	6.27108	-1.51247	3.59946	-2.1323	1.723

The inclusion of the fringing field into that of the quadrupoles follows exactly that of RAYTRACE[5] (POLES option).
The Dipole field calculation used the RAYTRACE based analytic model for dipoles with field gradient (MTYP = 4). Parameters were determined from the field mapping[4].
The model is used to generate a set of trajectories that fill the acceptance of the spectrometer. These trajectories are used as a database to determine, by fitting, the optical transfer coefficients of the spectrometers. This model of the spectrometer does a reasonably good job of describing the empirically determined spectrometer properties. In the table below a comparison is made between the empirically determined transfer coefficients and those determined using the model for the determination of δ.

Coefficient	Empirical	Model
D_{1000}	0.0853	0.0838
D_{2000}	0.0107	0.0110
D_{0100}	-0.0404	-0.0361
D_{1100}	0.26	0.25
D_{2100}	0.0362	0.0238
D_{3100}	0.1087	-0.0133
D_{0200}	-1.37	-1.68
D_{1200}	0.31	0.99
D_{2200}	-1.36	0.48
D_{0300}	36.7	-10.0
D_{1300}	-15.7	-14.8
D_{0002}	0.183	-0.109
D_{1002}	-0.22	0.38
D_{2002}	-0.32	0.20
D_{0020}	0.55	0.29
D_{1020}	0.65	-0.03
D_{2020}	0.78	0.12
D_{0011}	0.33	0.35
D_{1011}	1.16	0.21
D_{2011}	1.45	-0.57
D_{0120}	-0.53	-19.67
D_{1120}	10.1	7.6
D_{0102}	-8.3	-17.0
D_{1102}	-51	-3
D_{0111}	-52	-5
D_{1111}	-5.78	-23.21
D_{0400}	2187	1199
D_{0202}	-358	-348
D_{0220}	-424	-312
D_{0211}	-370	-6
D_{0040}	66	43
D_{0004}	-91	15
D_{0022}	249	41
D_{0031}	-257	49
D_{0013}	-162	-9

Monte Carlo Evaluation of Errors:

The determination of the impact of measurement errors on the resolution capabilities of the spectrometer are evaluated with a program called MUFIT. Beyond the simple description given above in the General Scheme Section, figure 2 illustrates how MUFIT works.

Figure 2

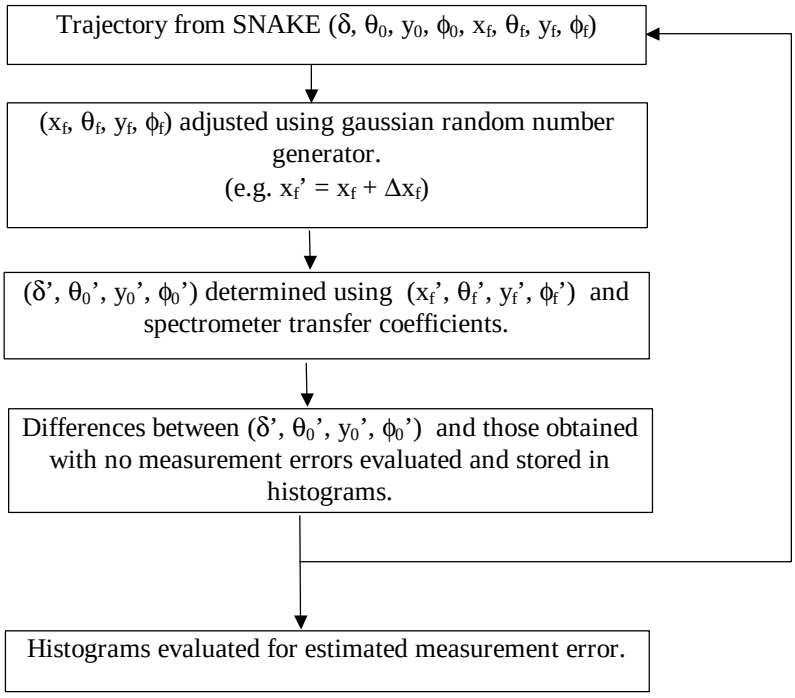

A representative set of histograms is shown in figure 3.

Summary

Figures 4-11 summarize the effect of multiple scattering at the spectrometer exit on momentum, position, and angular resolution. In particular a comparison is made between using the "standard" 4 mil Ti exit window and a much thinner "Mainz-style" window. The effect of things prior to the spectrometer are explicitly **not** included in this analysis. Things that would further decrease resolution include:

- Multiple scattering in the target material, target windows, and vacuum windows at the entrance to the spectrometer.
- Incident beam energy spread.
- Uncertainty in the beam position when the raster is on.
- Ionization energy loss effects. (These can depend strongly on target geometry and particulars of the experimental kinematics)
- …

In most cases, the combined effect of the above entrance effects will be at least as large as the effects of multiple scattering at the exit. Nevertheless, it appears on the basis of this analysis that there is little to gain by implementing the thin exit window.

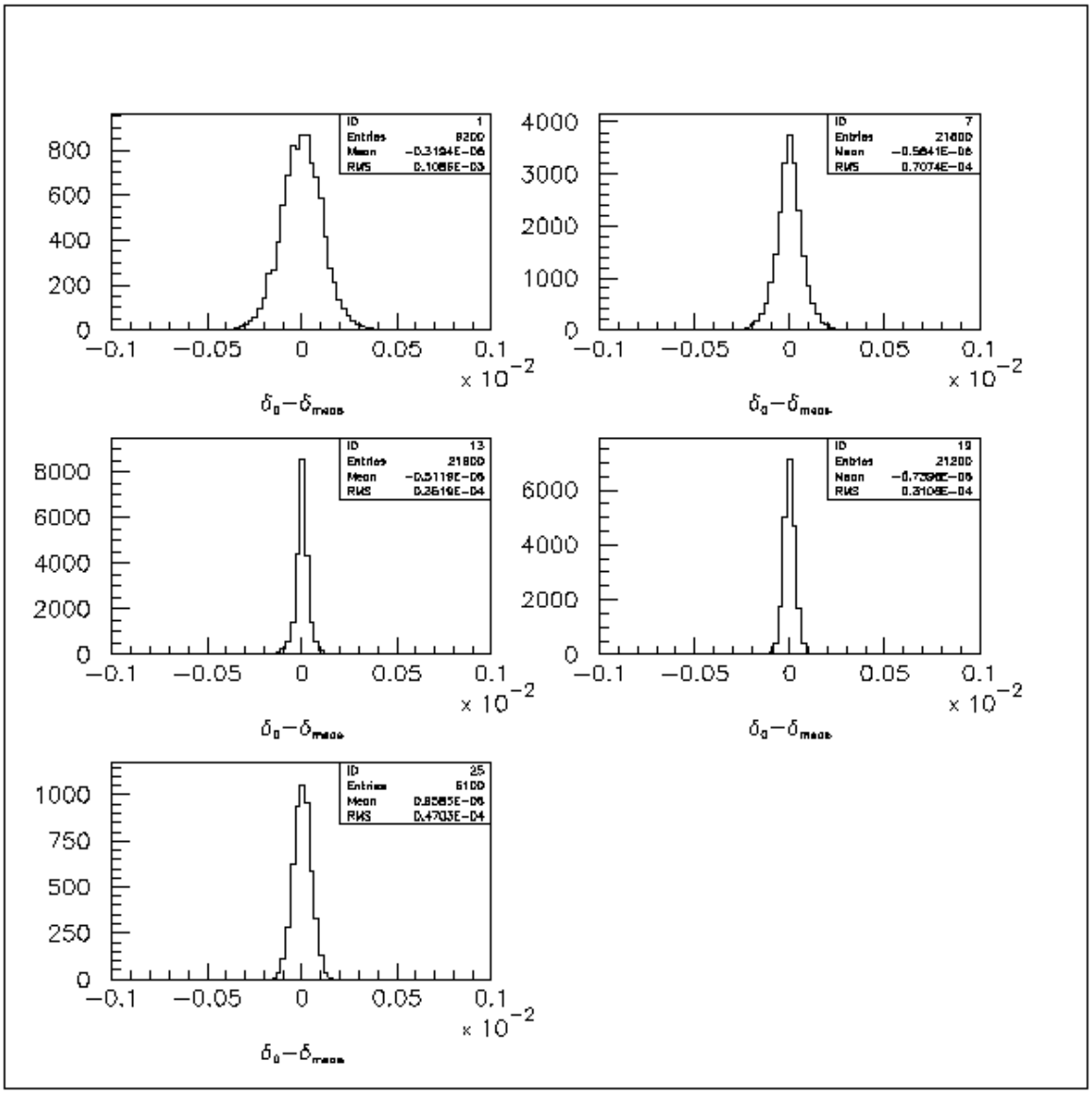

Figure 3: Histograms of δ resolution for 1GeV/c electrons with the 4 mil Ti window and standard detector package for various values of δ. ID = 1, 7, 13, 19, 25 are for δ = -4.5%, -2.25%, 0, 2.25%, 4.5% respectively.

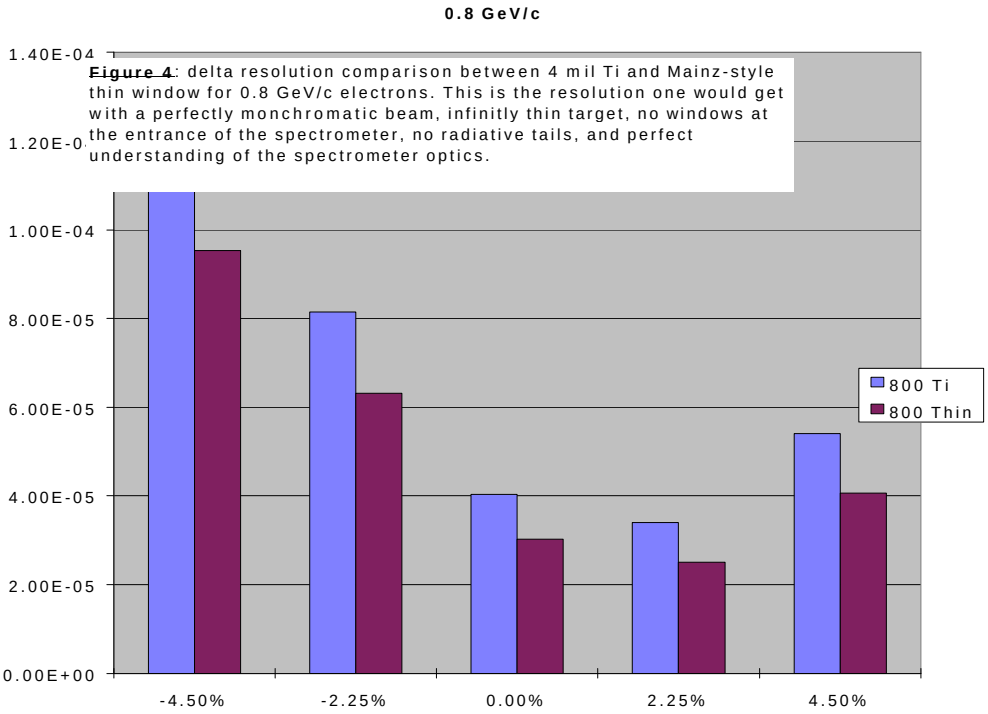

Figure 4: delta resolution comparison between 4 mil Ti and Mainz-style thin window for 0.8 GeV/c electrons. This is the resolution one would get with a perfectly monchromatic beam, infinitly thin target, no windows at the entrance of the spectrometer, no radiative tails, and perfect understanding of the spectrometer optics.

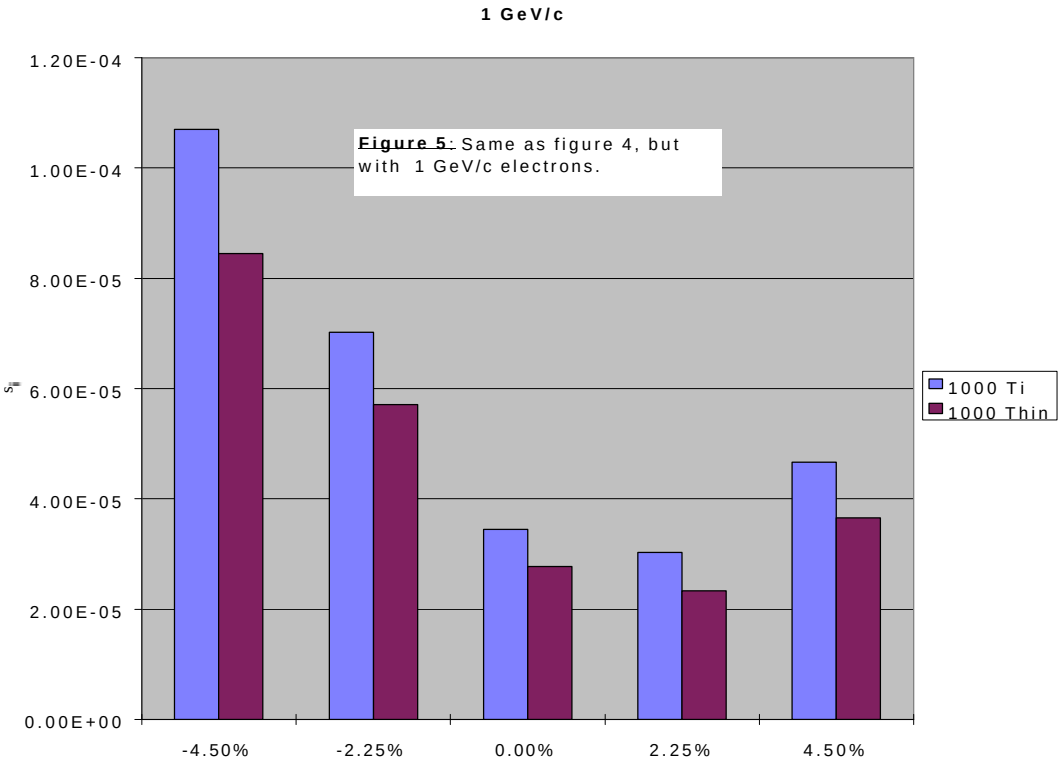

Figure 5: Same as figure 4, but with 1 GeV/c electrons.

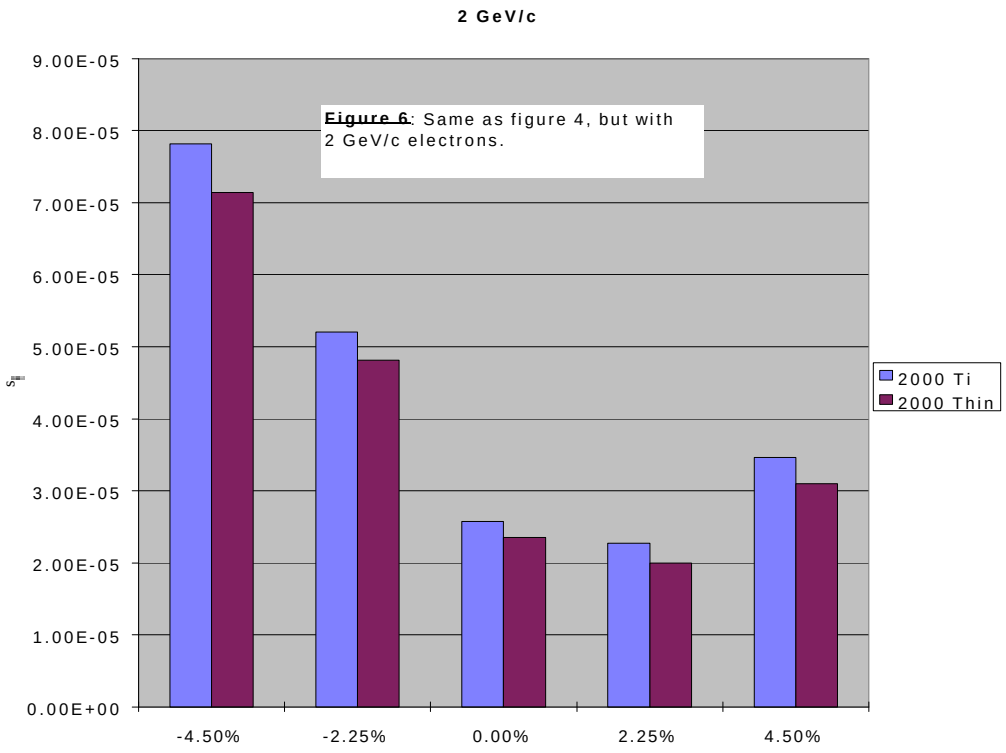

Figure 6: Same as figure 4, but with 2 GeV/c electrons.

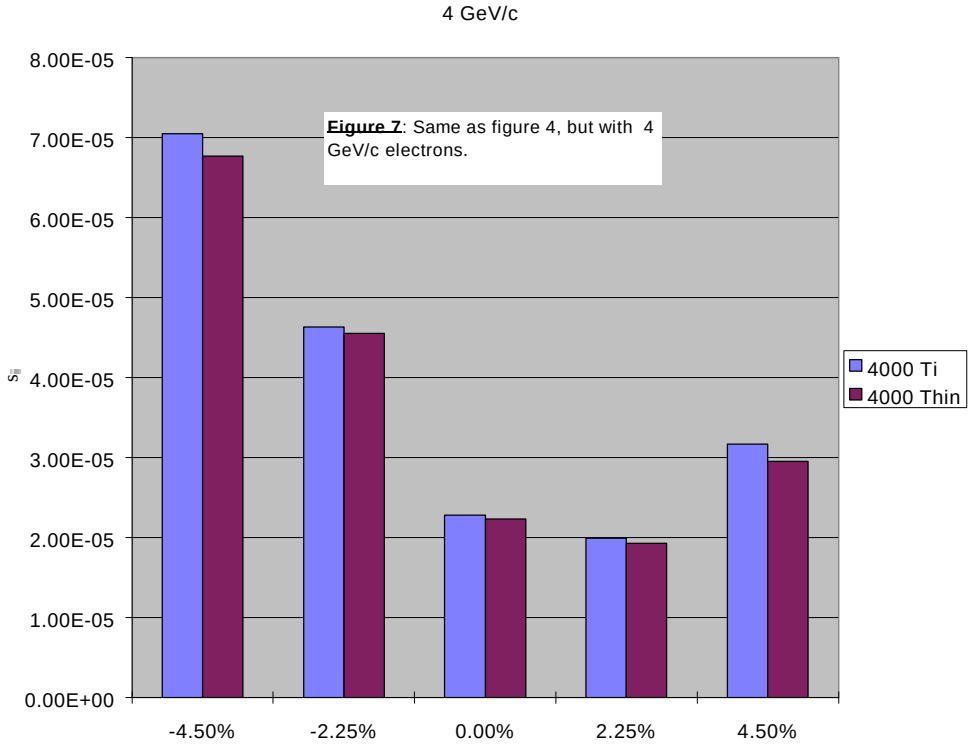

Figure 7: Same as figure 4, but with 4 GeV/c electrons.

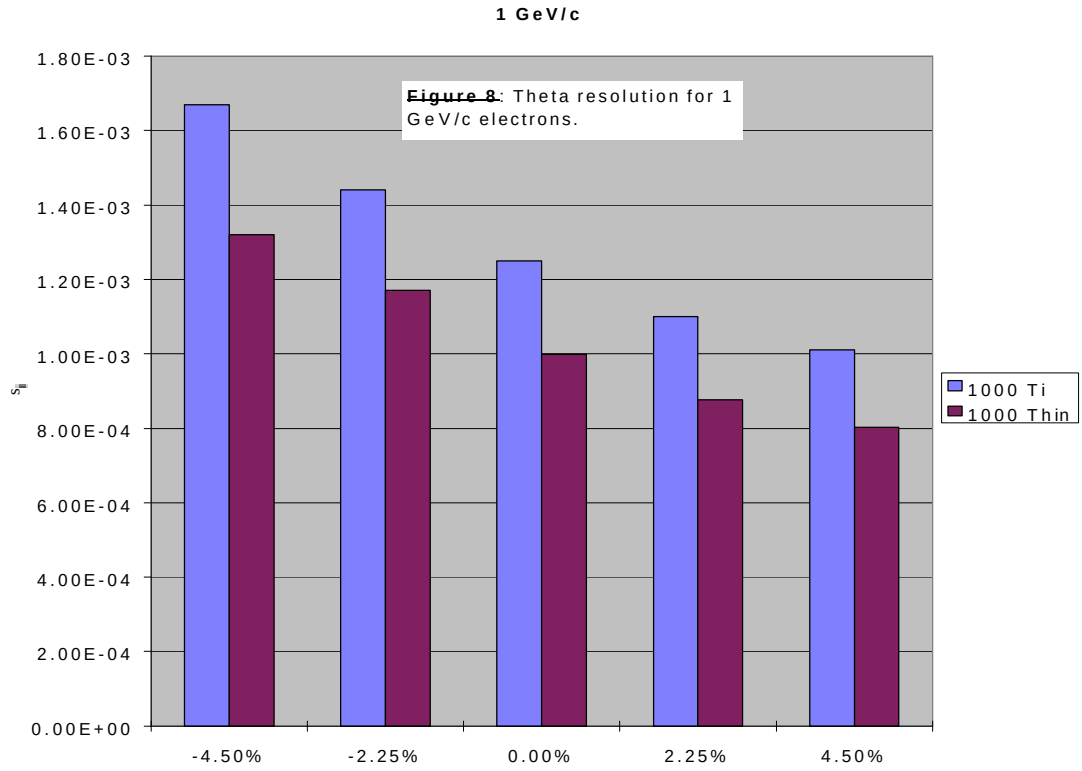

~~Figure 8~~: Theta resolution for 1 GeV/c electrons.

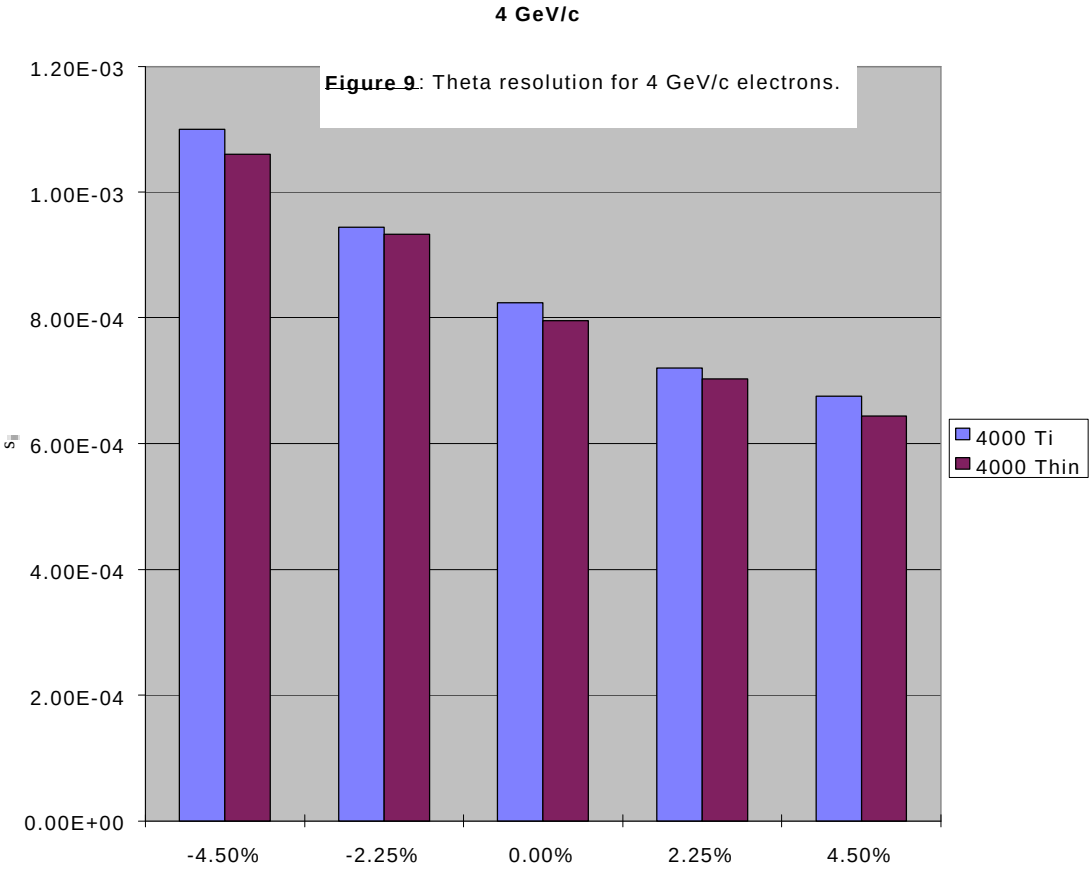

~~Figure 9~~: Theta resolution for 4 GeV/c electrons.

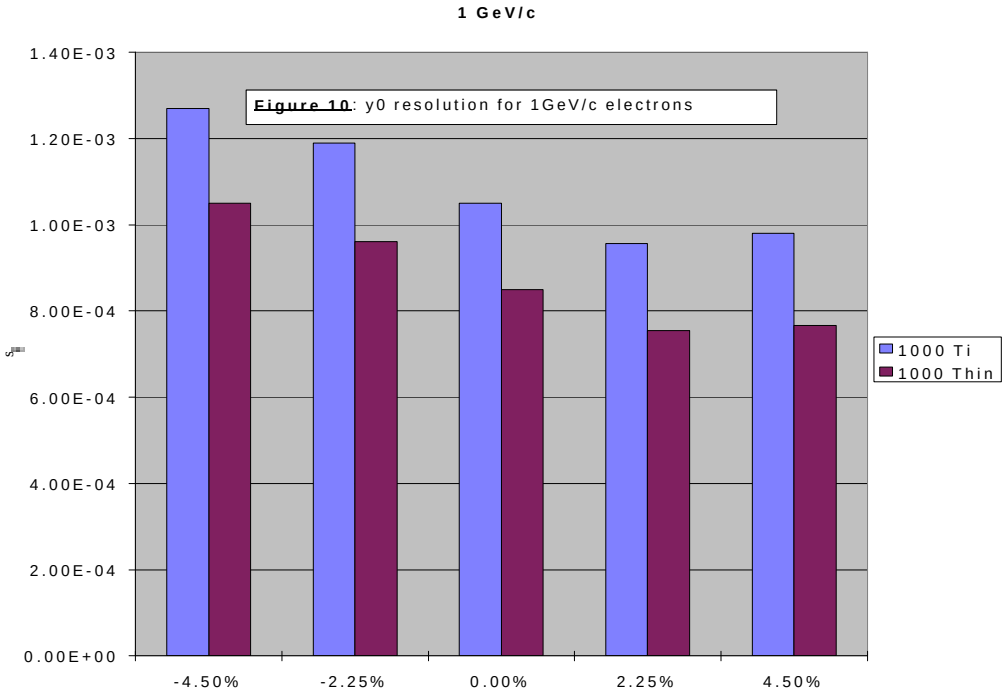

Figure 10: y0 resolution for 1GeV/c electrons

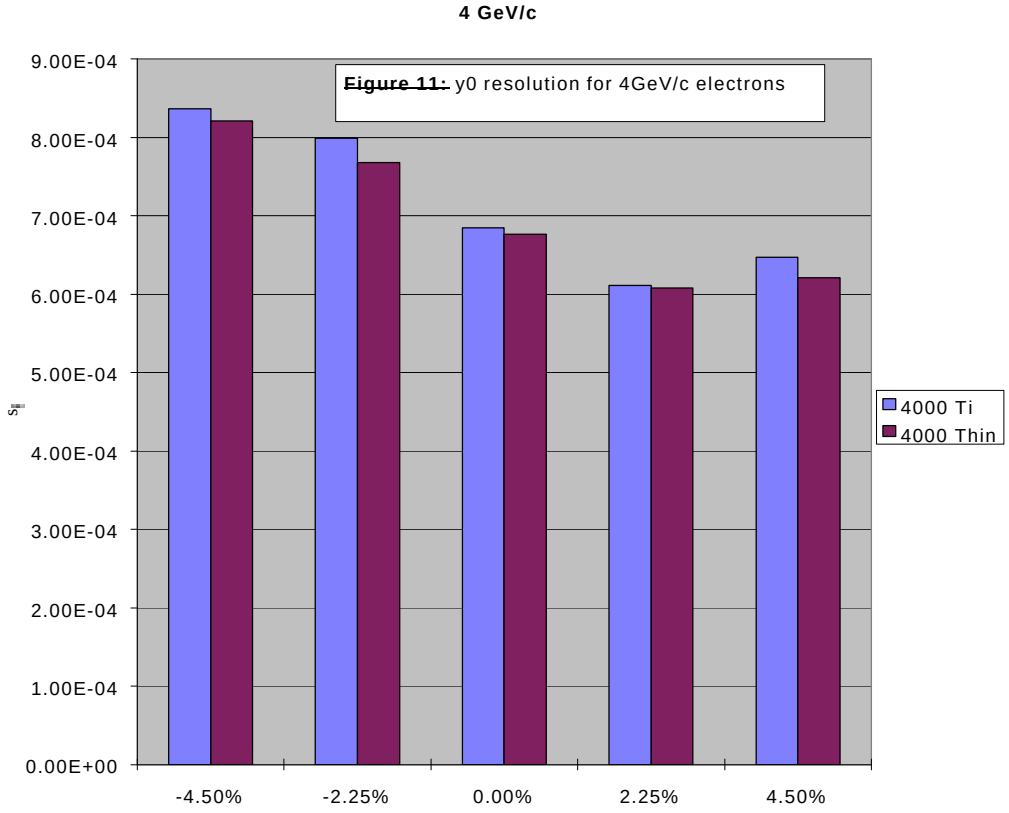

Figure 11: y0 resolution for 4GeV/c electrons

[1] R.M. Barnett et al., Physical Review **D54**, 1 (1996)
[2] JAHRESBERICHT 1992-1993, Institut für Kernphysik Johannes Gutenberg-Universität Mainz, p. 83
[3] SNAKE: Raytracing code developed primarily by Pascal Vernin.
[4] P. Vernin, et al., "Field Mapping of the High Resolution Spectrometers of JLab Hall A", submitted to NIM for publication.
[5] RAYTRACE, see RAYTRACE manual by S. Kowalski and H.A. ENGE, Laboratory for Nuclear Science and Department of Physics, MIT, 16 May 1986